

# Pivot burrowing of scarab beetle (*Trypoxylus dichotomus*) larva

Haruhiko Adachi (✉ [h.adachi@fbs.osaka-u.ac.jp](mailto:h.adachi@fbs.osaka-u.ac.jp))

Osaka University <https://orcid.org/0000-0002-9420-5335>

Makoto Ozawa

Osaka University

Satoshi Yagi

Osaka University

Makoto Seita

Osaka University

Shigeru Kondo

Graduate School of Frontier Biosciences, Osaka University, 1-3 Yamadaoka, Suita, Osaka 565-0871

---

## Brief Communication

**Keywords:** scarab beetle (*Trypoxylus dichotomus*) larvae, pivot burrowing, movement, adaptation

**Posted Date:** January 25th, 2021

**DOI:** <https://doi.org/10.21203/rs.3.rs-152830/v1>

**License:**   This work is licensed under a Creative Commons Attribution 4.0 International License.

[Read Full License](#)

---

**Version of Record:** A version of this preprint was published at Scientific Reports on July 16th, 2021. See the published version at <https://doi.org/10.1038/s41598-021-93915-0>.

# 1 **Pivot burrowing of scarab beetle (*Trypoxylus dichotomus*) larva**

2 Haruhiko Adachi<sup>1\*</sup>, Makoto Ozawa<sup>2</sup>, Satoshi Yagi<sup>2</sup>, Makoto Seita<sup>1</sup>, Shigeru Kondo<sup>1</sup>

3 <sup>1</sup> Graduate School of Frontier Bioscience, Osaka University, Suita, Osaka, 565-0871, Japan

4 <sup>2</sup> Graduate School of Engineering Science, Osaka University, Toyonaka, Osaka 560-8531, Japan

5 \* Corresponding author and address. E-mail: h.adachi@fbs.osaka-u.ac.jp

6

## 7 **Abstract**

8 Scarab beetle larvae do not have appendages to shovel soil and their trunk is thick compared to their body length; hence, their  
9 movement through the soil is perplexing. Here, we found that the last larval instars of *Trypoxylus dichotomus* burrow in two  
10 different ways, depending on the hardness of the soil. If the soil is soft, the larvae keep their body in a straight line and use  
11 longitudinal expansion and contraction; if the soil is hard, they flex and rotate their body. It is thought that the larvae adapt to  
12 diverse soil conditions using two different excavation methods.

13

14 The soil is home to many organisms, and how they move through soil has been studied in several species (e.g., rats, lizards,  
15 snakes, nematodes, eels, spiders, ants, earthworms) by analyzing the shape of their burrows or/and using X-ray scanning  
16 technology.<sup>1-11</sup> Among them, earthworms have attracted much attention as a research model because they can burrow through  
17 soil without appendages, and their dynamics have recently been elucidated via an observation system using transparent  
18 superabsorbent polymers.<sup>12</sup> Furthermore, applications of these excavation techniques are being developed.<sup>13-15</sup> Earthworm  
19 morphology seems to be suitable for burrowing in terms of the drag force from the soil, as their trunk is narrow compared to

20 their body length. However, the shape of some organisms in the soil is suitable for burrowing. For example, the larva of the  
21 scarab beetle (*Trypoxylus dichotomus*), which spend their life in the soil until adult emergence. Their trunk is very thick  
22 compared to their body length; the transverse sectional diameter of a earthworm is approximately 2 mm<sup>16</sup>, whereas that of the  
23 last instar larvae is ~20 mm. In other words, the transverse sectional area of beetle larvae contributing to resistance from the soil  
24 is almost 100 times larger than that of a earthworm. Therefore, there the burrowing mechanism must be different from that of  
25 earthworms under similar conditions. Although beetle ecology in the soil has been reported in several studies<sup>17,18</sup>, little is known  
26 about how beetle larvae move.

27

28 Here, we analyzed the burrowing mechanisms of beetle larvae. Beetle larvae were placed on the soil surface to make sure they  
29 could burrow into the soil (Figure 1A). In order to observe the burrowing behavior, a two-dimensional (2D) observation tank  
30 (130 × 210 × ~20 mm) was constructed (Figure 1B); we succeeded in observing the dynamics of the larvae under a 2D soil  
31 condition (Figure 1C, Supplementary Movie 1). The larvae burrowed by rotating themselves (Figure 1D, Supplementary Movie  
32 1). Rotation was observed regardless of sex. All observed individuals proceeded towards the bottom and stopped when rotating  
33 at the bottom layer (Figure 1C).

34 Next, we investigated whether the hardness of the medium being excavated could change the dynamics of burrowing. Different  
35 amounts of soil were used to compare compacted soil (relative volume of soil: 1) and non-compacted soil (relative volume of  
36 soil: 1/2). The speed of burrowing was faster (Figure 1D, Supplementary Movie 1) and the degree of rotation was smaller when  
37 burrowing in non-compacted soil (Figure 1D, Supplementary Movie 1). However, in these observation systems, there were  
38 several areas that could not be observed clearly to analyze the dynamics because the soil covered their body. Therefore, we

39 searched for a burrowing medium that would aid in observing the burrowing dynamics clearly. We constructed a complete 2D  
40 observation system by stacking cylindrical paper straws of two diameters cut into 2 cm segments (Figure 2A). By changing the  
41 diameter of the straw (using 6 mm and 10 mm diameter straws), the area of the lumen changes, which is thought to have the  
42 similar effect as soil compaction changes.

43 As a result, we could observe quite clearly how the burrowing larvae rotate. Through the 6 mm straws, the larvae proceeded  
44 towards the bottom by rotating and stopped at the bottom layer just as in the hard soil (Fig. 2C, Supplementary Movie 3). The  
45 larvae were seen to rise to the surface without moving to the bottom layer through the 10 mm straws, contrary to in the soft soil  
46 (Fig. 2D, Supplementary Movie 5). Although beetle larvae are known to be able to change their burrowing direction depending  
47 on CO<sub>2</sub> concentration<sup>17</sup>, their movement may also be motivated by the size of the surrounding particles or by sensing other  
48 factors that vary with size.

49 We analyzed the movie of larval dynamics using Fiji's Plugin "manual tracking" (version 1.0). Beetle larvae have nine  
50 spiracles, which were used as indicators in the tracking analysis (Fig. 2B, E, F, S1, Supplementary Movie 4 and 6) (some parts,  
51 where the spiracles were not visible, were skipped.). Larvae could twist and turn their bodies in the 2D environment (Fig. 2E,  
52 red arrow). We first investigated the velocity of the spiracles. Movement of anterior parts was faster than posterior parts and the  
53 velocity in the 10 mm cylinder was faster than in the 6 mm cylinder (Fig. 2G). This velocity tendency (6 mm vs 10 mm)  
54 corresponds to the tendency in the soil compaction experiment (with vs without compaction). In addition, the change in angle  
55 between the three spiracles (3,5,9) was measured (Fig. 2H). Although there were two peak angles under both straw medium  
56 conditions, the position of the peaks was different. In 6 mm straws, the first peak was ~80° and the second peak was ~130°. In  
57 10 mm straws, the peaks were at ~90° and ~150°. The frequency of the peaks was also different. In 10 mm straws, the first peak

58 distribution was less than in 6 mm. The two peaks indicate two modes of larval shape; the first peak indicates C-shaped shape,  
59 and the second peak indicates straight shape. It is assumed that there exists a relationship between larval shape and the presence  
60 or absence of pivot movement. Hence, the larval pivot burrowing can be changed depending on the surrounding environment.

61 From the experiments with different soil contents and different straw diameters, a correlation between velocity and the degree  
62 of rotation was evident. If the environment was conducive to fast progress, the larva went straight ahead; if not, they rotated.

63 Next, we examined the relationship between rotation position and larval shape. To investigate the location of rotation, we  
64 plotted the time transition of the Y-position of spiracle 3. With rotation, the Y-position fluctuated up and down periodically.

65 Time series data of the angle were plotted. Angle and Y-position were inversely related (Fig. 2I, S2). This suggests that  
66 rotational burrowing may contribute to the larvae pushing (kicking) the soil with their tails to move downward (Fig. 2J).

67 Another possible reason is that the rotation and pivoting motion causes local fluidization of the soil, thereby reducing the  
68 resistance.<sup>19</sup> The reason for the lack of a clear inverse relationship before reaching a certain depth is thought to be that the straw  
69 was not heavy enough to provide a drag force when pushed with the buttocks. Movement by pushing of the tail has been  
70 reported in tiger beetle larvae.<sup>20</sup> Although the tiger beetle larvae also burrow in the soil,<sup>21,22</sup> the shape of the hole is straight, and  
71 it is assumed that they do not burrow with rotation like the scarab beetle larvae. The tiger beetle larvae are not C-shaped like the  
72 scarab beetle larvae.<sup>21,22</sup> There is a possibility that larval morphology may cause rotation. In the future, comparisons with the  
73 tiger beetle can facilitate ecological evolutionary developmental biology (Eco-Evo-Devo) research.

74

75 In this study, we established a 2D observation system for beetle larvae and analyzed how they move. As a result, we discovered  
76 that scarab beetle larvae burrow by rotating. Burrowing dynamics changed when the hardness and size of the soil particles were

77 changed. In addition, the relationship between larval shape and timing of rotation was clarified, suggesting that rotated  
78 movement may be conducive to displacing the soil to move downwards. A 2D observation system was used in this study; it is  
79 unclear whether the same behavior would be observed in a 3D environment. X-ray CT technology would facilitate the  
80 reconstruction of images in a short time, which would elucidate burrowing dynamics. The rotational movement may be an  
81 effective way of burrowing by repeating simple movements. The significance of this rotational motion needs to be confirmed by  
82 reproducing it in a robot. Few studies have investigated the development of excavation robots that apply the burrowing  
83 mechanisms of animals (e.g., inchworms, shellfish, and earthworms).<sup>15,23-25</sup> The application of the burrowing mechanism of  
84 beetle larvae may also contribute to the development of new excavation technologies.

85 The rotational movement is caused by the shape of the larvae. Comparison of the larvae with those of other soil insects, such as  
86 the tiger beetle larvae<sup>21,22</sup>, which burrows linearly, would facilitate Eco-Evo-Devo research. Additionally, the results of studies  
87 on the frequency, position, and direction of the rotation can be applied in the field of neuroethology.

88

## 89 **Materials and Methods**

### 90 **Insects**

91 The last instars of Japanese rhinoceros beetle (*Trypoxylus dichotomus*) were commercially purchased (Finebeetle, Ehime, Japan)  
92 and kept individually in 500–1000 mL bottles filled with rotted wood flakes at 10–15 °C until use.

### 93 **Observation of burrowing**

94 The larvae were moved to a room with a temperature of 23 °C and could acclimatize for at least 30 min before the burrowing  
95 experiment was conducted. Larval movements in the glass tank (6 × 21 × 2 cm) were captured by a time-lapse camera

96 (DMCGX7MK2WK, Panasonic, Osaka, Japan). The larvae were incubated in a humus mat (Kanzen, Tsukinoyakinokoen,  
97 Gunma, Japan) and paper straws (6 mm, Shimojima, Tokyo, Japan) (10 mm, Zone Plus, Shiga, Japan) were cut into ~2 cm  
98 pieces for visualization.

### 99 **Analysis of tracking**

100 From the data obtained by time-lapse photography, the coordinates of the spiracles present in each body segment of the larvae  
101 were obtained for each time series using Fiji's macro manual tracking (version1.0). The data were skipped when the spiracles  
102 were unclear. Based on the size of the tank, the distance per pixel was calculated and used for subsequent determination of  
103 velocity between the spiracles. In the time lapse, the images were taken every second, so the displacement of each image of each  
104 trachea was directly used as the velocity. The angle was calculated from the positional information of the three spiracles. All  
105 analysis after obtaining the positional information was done in Julia language (version1.5).

106

### 107 **Acknowledgement**

108 We acknowledge Dr. Seita Miyazawa (Osaka University) for providing tools and helpful comment. We acknowledge Dr.  
109 Hiroki Gotoh (National Institute of Genetics) and Dr. Nobuyuki Noda (Advanced Telecommunications Research Institute), and  
110 Dr. Kyosuke Adachi (RIKEN Center for Biosystems Dynamics Research) for helpful comment. We acknowledge the members  
111 of Shigeru Kondo's Laboratory (Osaka University) for providing a comfortable environment for research and helpful  
112 discussion.

113

### 114 **Competing interests**

115 The authors declare no competing interests.

116

### 117 **Author contributions**

118 Conceptualization: H.A.; Methodology: H.A., M.O., S.Y. and S.K.; Validation: H.A., M.O., S.Y. and S.K.; Formal analysis:

119 H.A.; Investigation: H.A.; Visualization: H.A.; Writing – original draft: H.A. and S.K.; Writing – review & editing: H.A., M.O.,

120 S.Y., M.S. and S.K.; Supervision: H.A. and S.K.; Project administration: H.A. and S.K.; Funding acquisition: H.A. and S.K.

121

### 122 **Funding**

123 This research was supported in part by the “Program for Leading Graduate Schools” of the Ministry of Education, Culture,

124 Sports, Science and Technology, Japan, and a grant from Leave a Nest Co. Ltd.

125

### 126 **References**

127 1 Maladen, R. D., Ding, Y., Li, C. & Goldman, D. I. Undulatory Swimming in Sand: Subsurface Locomotion of the

128 Sandfish Lizard. *Science* **325**, 314-318, doi:10.1126/science.1172490 (2009).

129 2 Maladen, R. D., Ding, Y., Umbanhowar, P. B., Kamor, A. & Goldman, D. I. Mechanical models of sandfish locomotion

130 reveal principles of high performance subsurface sand-swimming. *Journal of the Royal Society Interface* **8**, 1332-1345,

131 doi:10.1098/rsif.2010.0678 (2011).

132 3 Sharpe, S. S. *et al.* Locomotor benefits of being a slender and slick sand swimmer. *Journal of Experimental Biology* **218**,

133 440-450, doi:10.1242/jeb.108357 (2015).

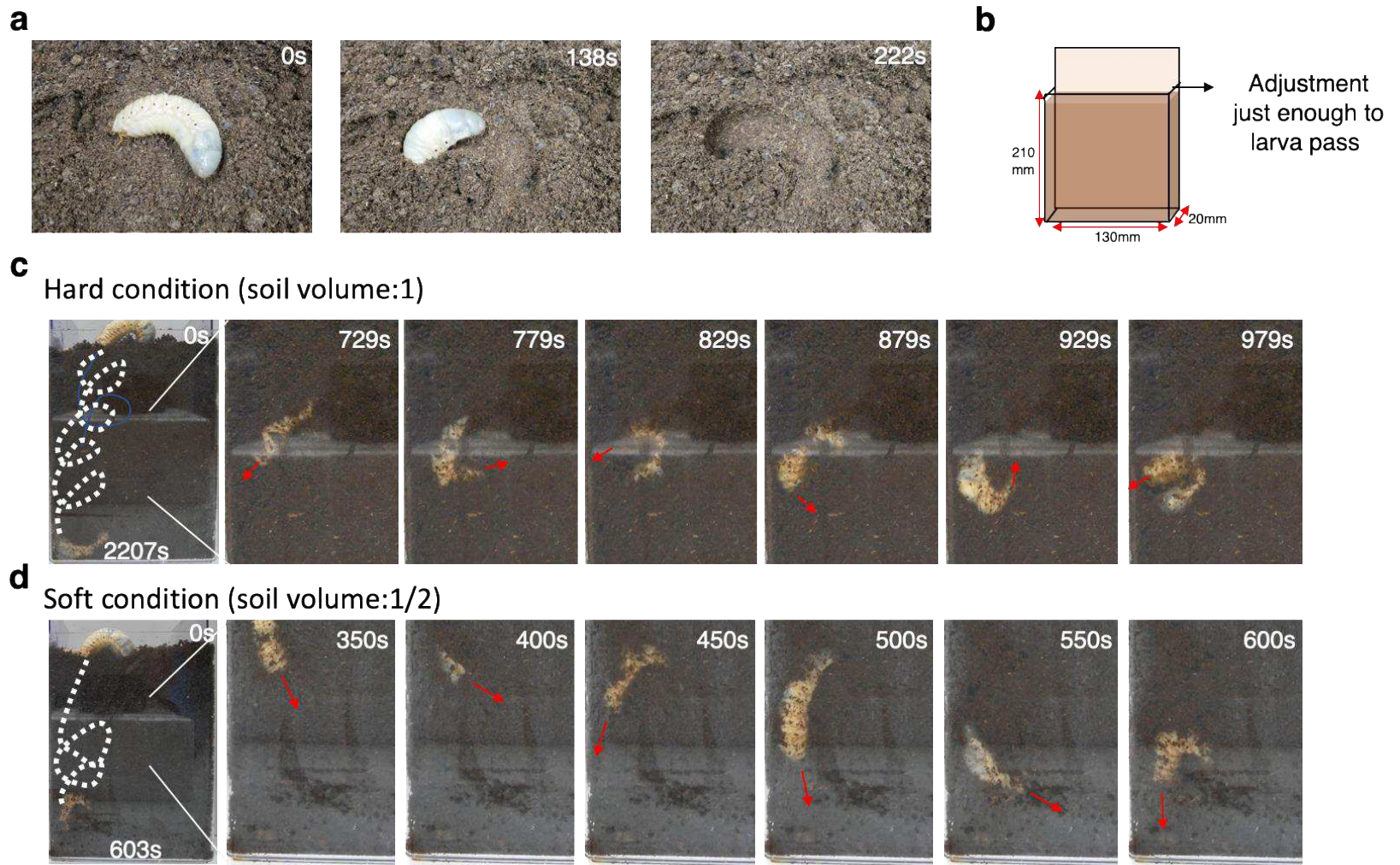
- 134 4 Jung, S. *Caenorhabditis elegans* swimming in a saturated particulate system. *Physics of Fluids* **22**,  
135 doi:10.1063/1.3359611 (2010).
- 136 5 Herrel, A. *et al.* Burrowing and subsurface locomotion in anguilliform fish: behavioral specializations and mechanical  
137 constraints. *Journal of Experimental Biology* **214**, 1379-1385, doi:10.1242/jeb.051185 (2011).
- 138 6 Hils, J. M. & Hembree, D. I. Neoichnology of the burrowing spiders *Gorgyrella inermis* (Mygalomorphae: Idiopidae)  
139 and *Hogna lenta* (Araneomorphae: Lycosidae). *Palaeontologia Electronica* **18** (2015).
- 140 7 Monaenkova, D. *et al.* Behavioral and mechanical determinants of collective subsurface nest excavation. *Journal of*  
141 *Experimental Biology* **218**, 1295-1305, doi:10.1242/jeb.113795 (2015).
- 142 8 Joschko, M. *et al.* A non-destructive method for the morphological assessment of earthworm burrow systems in three  
143 dimensions by X-ray computed tomography. *Biology and Fertility of Soils* **11**, 88-92, doi:doi:10.1007/BF00336369  
144 (1991).
- 145 9 Jégou, D., Cluzeau, D., Wolf, H. J., Gandon, Y. & Tréhen, P. Assessment of the burrow system of *Lumbricus terrestris*,  
146 *Aporrectodea giardi*, and *Aporrectodea caliginosa* using X-ray computed tomography. *Biology and Fertility of Soils* **26**,  
147 116-121, doi:doi:10.1007/s003740050353 (1997).
- 148 10 Jégou, D., Hallaire, V., Cluzeau, D. & Tréhen, P. Characterization of the burrow system of the earthworms *Lumbricus*  
149 *terrestris* and *Aporrectodea giardi* using X-ray computed tomography and image analysis. *Biology and Fertility of Soils*  
150 **29**, 314-318, doi:doi:10.1007/s003740050558 (1999).
- 151 11 Booth, S. G., Kurtz, B., Heer, M. I. d., Mooney, S. J. & Sturrock, C. J. Tracking wireworm burrowing behaviour in soil  
152 over time using 3D X-ray Computed Tomography. *undefined* (2020).

- 153 12 Kudrolli, A. & Ramirez, B. Burrowing dynamics of aquatic earthworms in soft sediments. *Proceedings of the National*  
154 *Academy of Sciences of the United States of America* **116**, 25569-25574, doi:10.1073/pnas.1911317116 (2019).
- 155 13 Kubota, T., Nagaoka, K., Tanaka, S., Nakamura, T. & Ieee. Earth-worm typed drilling robot for subsurface planetary  
156 exploration. *2007 Ieee International Conference on Robotics and Biomimetics, Vols 1-5*, 1394-+,  
157 doi:10.1109/robio.2007.4522368 (2007).
- 158 14 Tadami, N. *et al.* in *IEEE/RSJ International Conference on Intelligent Robots and Systems (IROS) / Workshop on*  
159 *Machine Learning Methods for High-Level Cognitive Capabilities in Robotics*. 4950-4955 (2017).
- 160 15 Isaka, K. *et al.* Development of Underwater Drilling Robot Based on Earthworm Locomotion. *Ieee Access* **7**, 103127-  
161 103141, doi:10.1109/access.2019.2930994 (2019).
- 162 16 Quillin, K. J. Kinematic scaling of locomotion by hydrostatic animals: Ontogeny of peristaltic crawling by the  
163 earthworm *Lumbricus terrestris*. *Journal of Experimental Biology* **202**, 661-674 (1999).
- 164 17 Kojima, W. Attraction to Carbon Dioxide from Feeding Resources and Conspecific Neighbours in Larvae of the  
165 Rhinoceros Beetle *Trypoxylus dichotomus*. *Plos One* **10**, doi:10.1371/journal.pone.0141733 (2015).
- 166 18 Kojima, W., Takanashi, T. & Ishikawa, Y. Vibratory communication in the soil: pupal signals deter larval intrusion in a  
167 group-living beetle *Trypoxylus dichotoma*. *Behavioral Ecology and Sociobiology* **66**, 171-179, doi:10.1007/s00265-011-  
168 1264-5 (2012).
- 169 19 Winter, A. G., Deits, R. L. H. & Hosoi, A. E. Localized fluidization burrowing mechanics of *Ensis directus*. *Journal of*  
170 *Experimental Biology* **215**, 2072-2080, doi:10.1242/jeb.058172 (2012).

- 171 20 Harvey, A. & Zukoff, S. Wind-Powered Wheel Locomotion, Initiated by Leaping Somersaults, in Larvae of the  
172 Southeastern Beach Tiger Beetle (*Cicindela dorsalis media*). *Plos One* **6**, doi:10.1371/journal.pone.0017746 (2011).
- 173 21 Gilbert, C. VISUAL DETERMINANTS OF ESCAPE IN TIGER BEETLE LARVAE (CICINDELIDAE). *Journal of*  
174 *Insect Behavior* **2**, 557-574, doi:10.1007/bf01053354 (1989).
- 175 22 Shelford, V. E. Life-Histories and Larval Habits of the Tiger Beetles (Cicindelidæ). *Journal of the Linnean Society of*  
176 *London, Zoology* **30**, 157-184, doi:10.1111/j.1096-3642.1908.tb02131.x (1908).
- 177 23 Zhang, W. W. *et al.* Development of an Inchworm-type Drilling Test-bed for Planetary Subsurface Exploration and  
178 Preliminary Experiments. *2016 Ieee International Conference on Robotics and Biomimetics (Robio)*, 2187-2191 (2016).
- 179 24 Winter, V. A. G. *et al.* in *IEEE/RSJ International Conference on Intelligent Robots and Systems.* (2010).
- 180 25 Koller-Hodac, A. *et al.* in *IEEE International Conference on Robotics and Automation (ICRA).* 1209-1214 (2010).

181

182



183

184 **Figure 1. Burrowing dynamics of scarab beetle (*Trypoxylus dichotomus*) larva**

185 (a) Burrowing images. After beetle is put on the soil, they can burrow in a short time (< 4 min). (b) A schematic of the pseudo-

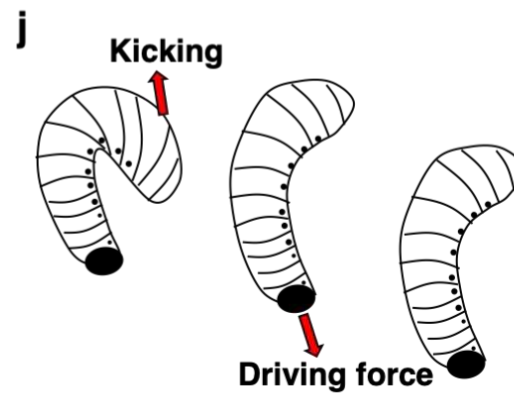
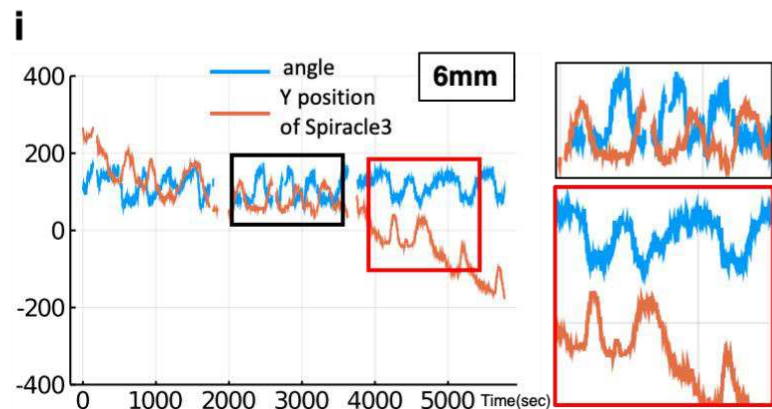
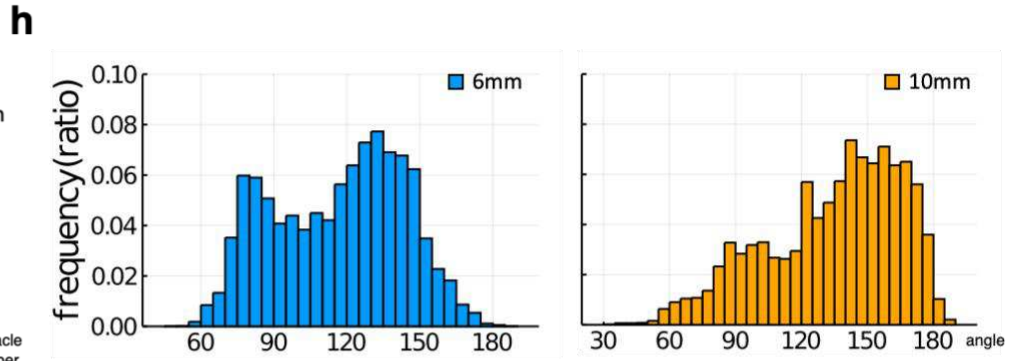
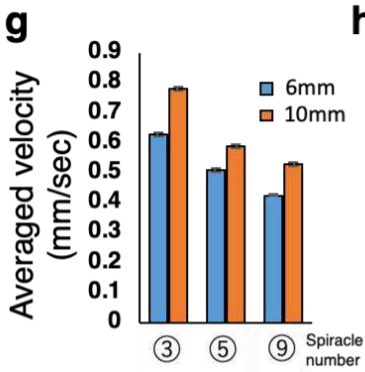
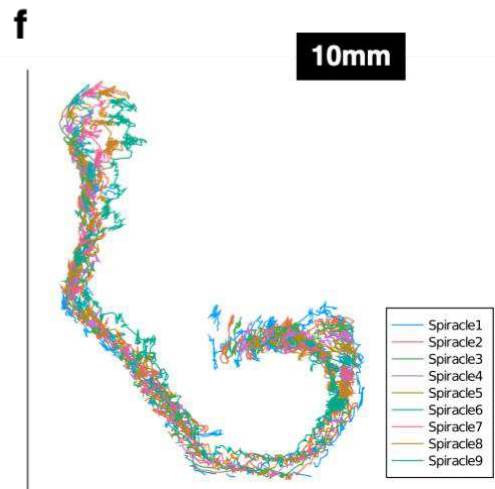
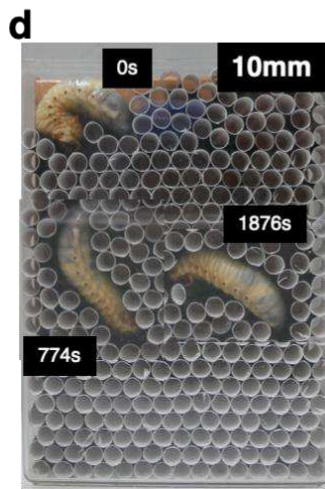
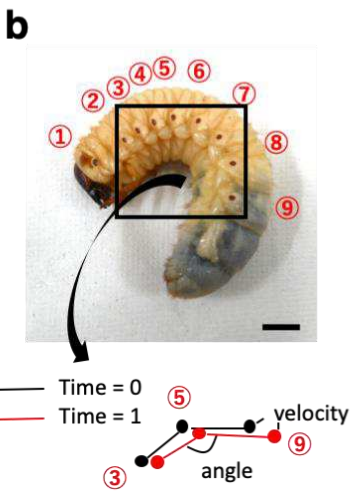
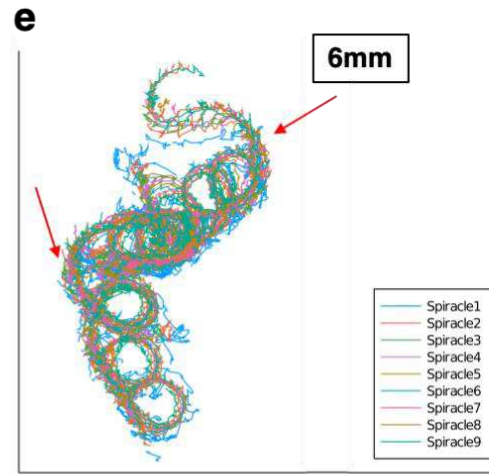
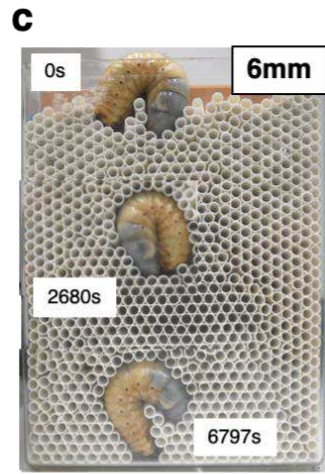
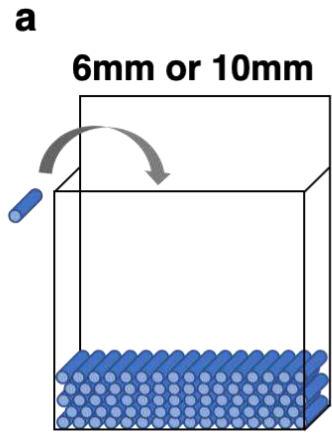
186 two dimensional (2D) observation tank. The depth was adjusted just enough for larva to pass. (c) Pseudo 2D observation image,

187 before and after burrowing, and during burrowing. (d) The dynamics of burrowing in soft sediment (half volume soil compared

188 to (c)).

189

190



192 **Figure 2. Observation system to analyze burrowing movement of scarab beetle (*Trypoxylus dichotomus*) larvae**

193 **(a)** A schematic of the pseudo two-dimensional (2D) observation system for analysis. Cut paper straws were stacked up. **(b)**

194 Tracking analysis scheme. Nine spiracles were tracked by the ImageJ plugin “manual tracking” (Version 1.0) from three

195 animals in each experiment. The angle was calculated from three spiracles (3,5,9).

196 **(c and d)** Pseudo 2D observation image burrowing in 6 mm and 10 mm cylinders. **(e and f)** The trajectory of nine spiracles

197 burrowing in 6 mm and 10 mm cylinders. Red arrows show the twisting and turning points. **(g)** The average velocity of the

198 spiracle in 6 mm and 10 mm cylinders. **(h)** The histogram of the angle calculated from three spiracles (3,5,9) in 6 mm and 10

199 mm cylinders from three beetle movement. **(i)** Relationship between rotation and the velocity of spiracle 3 in 6 mm cylinders.

200 Blue line shows the angle calculated from three spiracles (3,5,9), and the orange line shows the vertical position of spiracle 3

201 each time. (Other data in the 6 mm cylinders and 10 mm cylinders are in Fig. S2).

202

# Figures

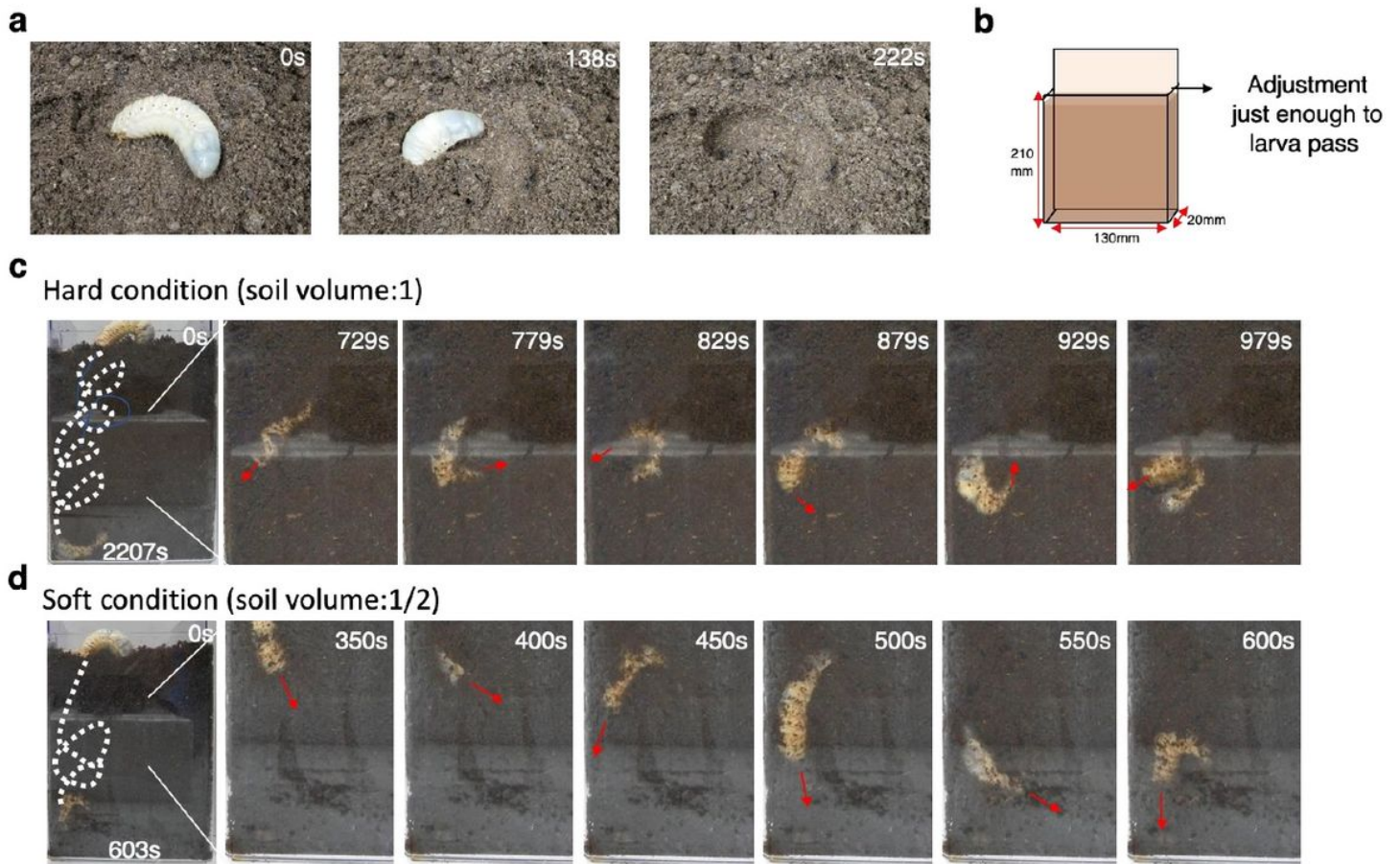


**Figure 1**

Burrowing dynamics of scarab beetle (*Trypoxylus dichotomus*) larva (a) Burrowing images. After beetle is put on the soil, they can burrow in a short time ( $< 4$  min). (b) A schematic of the pseudo- two dimensional (2D) observation tank. The depth was adjusted just enough for larva to pass. (c) Pseudo 2D observation image, before and after burrowing, and during burrowing. (d) The dynamics of burrowing in soft sediment (half volume soil compared to (c)).

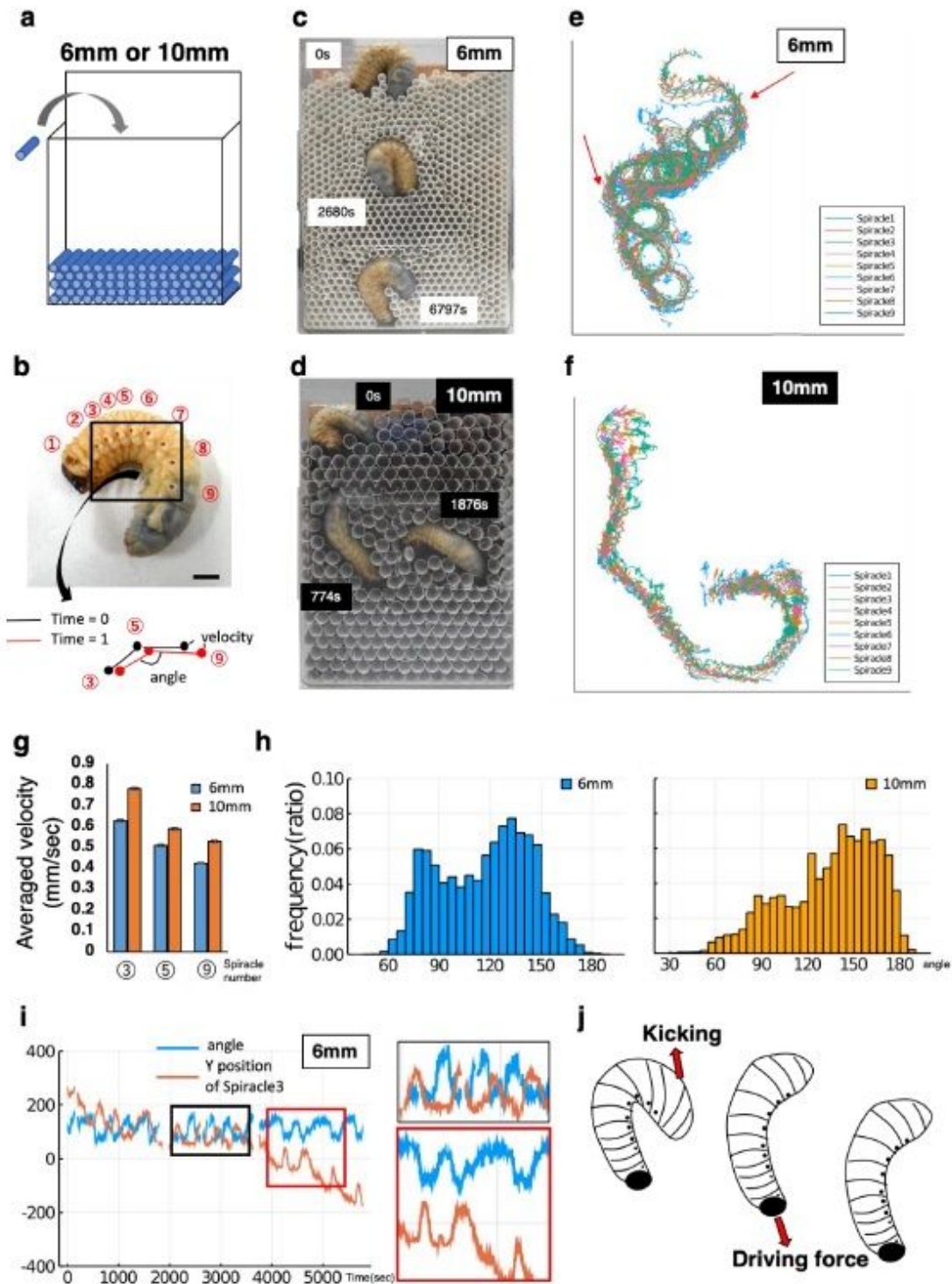


**Figure 2**

Observation system to analyze burrowing movement of scarab beetle (*Trypoxylus dichotomus*) larvae (a) A schematic of the pseudo two-dimensional (2D) observation system for analysis. Cut paper straws were stacked up. (b) Tracking analysis scheme. Nine spiracles were tracked by the ImageJ plugin “manual tracking” (Version 1.0) from three animals in each experiment. The angle was calculated from three spiracles (3,5,9). (c and d) Pseudo 2D observation image burrowing in 6 mm and 10 mm cylinders. (e and

f) The trajectory of nine spiracles burrowing in 6 mm and 10 mm cylinders. Red arrows show the twisting and turning points. (g) The average velocity of the spiracle in 6 mm and 10 mm cylinders. (h) The histogram of the angle calculated from three spiracles (3,5,9) in 6 mm and 10 mm cylinders from three beetle movement. (i) Relationship between rotation and the velocity of spiracle 3 in 6 mm cylinders. Blue line shows the angle calculated from three spiracles (3,5,9), and the orange line shows the vertical position of spiracle 3 each time. (Other data in the 6 mm cylinders and 10 mm cylinders are in Fig. S2).

## Supplementary Files

This is a list of supplementary files associated with this preprint. Click to download.

- [supplimentpivotburrowing.pdf](#)
- [SupplementaryMovie1.mov](#)
- [SupplementaryMovie2.mov](#)
- [SupplementaryMovie3.mov](#)
- [SupplementaryMovie4.avi](#)
- [SupplementaryMovie5.mov](#)
- [SupplementaryMovie6.avi](#)